375

Buoyancy-driven flow between parallel plane vertical walls

W.H.H. BANKS and M.B. ZATURSKA
School of Mathematics, University of Bristol, Bristol BS8 1TW, UK

Abstract. We examine theoretically the two-dimensional free-convective flow in a parallel-walled cell with vertical walls at non-uniform temperature; this temperature variation is such that similarity solutions for the flow and temperature fields are possible. Both symmetric and asymmetric boundary conditions are considered. In the former case we find that in addition to a trivial symmetric solution, corresponding to stagnant flow, there are non-trivial steady symmetric solutions and also steady asymmetric solutions for certain ranges of Rayleigh number. The temporal stability of all these solutions is also investigated and the nature of the bifurcations examined; these include bifurcations of pitchfork, transcritical and Hopf types. The breaking of symmetry is studied and also the effect on the flow character of different Prandtl numbers.

1. Introduction

The use of a fluid as a coolant for industrial purposes has a long history. In most cases the coolant is forced over a hot solid surface which is cooled as a result. In other cases the fluid motion is generated because the fluid nearer the hotter region becomes lighter and so gives rise to what is termed natural or free convection. In both cases the underlying function of the moving fluid is to disperse the heat although the efficacy of such heat transfer is greatly enhanced with forced convection. However, we should remark that when rotation is present, so as to increase the body force, the heat transfer can be significantly increased (Schmidt [1]).

It is not uncommon in some cases to construct a series of fins projecting from the hot surface in order to enhance the transfer of heat. More topically, natural convection cooling is also important in electronic cabinets containing circuit cards: the cards are so aligned as to form vertical channels; see Said and Krane [2] and also for further references. With this in mind we have, in this paper, focussed attention on the two-dimensional free-convective flow in a cell formed by such fins or cards. Because of the cooling nature of such flows we model the physical problem by specifying the non-constant temperature on the cell walls; this is done in a particular way so that a similarity solution is possible which results, when the flow is steady, in the Navier–Stokes and temperature equations being reduced to a sixth-order system of ordinary differential equations. The problem contains three parameters: Ra, the Rayleigh number, Pr, the Prandtl number and μ, a parameter which measures the asymmetry of the imposed temperature on the cell walls. We note that problems involving free convection in tubes have been studied by Lighthill [3] and by Ostrach and Thornton [4].

When $\mu = 1$ the problem is symmetrical about the central plane of the cell although we show that in addition to symmetrical solutions there are asymmetric solutions for a range of Rayleigh numbers. We also show for this value of μ that, for all Ra, in addition to the trivial (stagnant) symmetric solution, there is a non-trivial symmetric solution: we find that on this solution branch the temperature becomes singular (blow-up) for Ra = 0, although the flow velocities remain finite.

We also formulate the eigenvalue problem that governs the temporal stability of such flows and we are able to categorise the solutions found into stable and unstable flows. In so doing we also show the presence of a Hopf bifurcation and, as a result, we infer the existence of periodic solutions.

Finally, we consider the effects of a cell with asymmetrically heated walls corresponding to $\mu \neq 1$. We obtain certain characteristics including the loci of some of the bifurcation points which delineate the regions of stability and of the periodic solutions.

2. Formulation of the problem

Consider the unsteady flow of an incompressible fluid with velocity field **u** and temperature field T. The equation governing the motion when the fluid properties are constant can be written

$$\frac{\partial \boldsymbol{\omega}}{\partial t} + \mathbf{u} \cdot \nabla \boldsymbol{\omega} = \boldsymbol{\omega} \cdot \nabla \mathbf{u} + \nabla \times \mathbf{F} + \nu \nabla^2 \boldsymbol{\omega} \, , \tag{2.1}$$

where t denotes time, $\boldsymbol{\omega} = \nabla \times \mathbf{u}$ is the vorticity, **F** is the body force and ν the kinematic viscosity of the fluid. The equation of continuity for an incompressible fluid is

$$\nabla \cdot \mathbf{u} = 0 \tag{2.2}$$

and the temperature field satisfies

$$\frac{\partial T}{\partial t} + \mathbf{u} \cdot \nabla T = \alpha \nabla^2 T \, , \tag{2.3}$$

where α is the thermal diffusivity of the fluid. Viscous dissipation has been neglected. The fluid motion results solely from the buoyancy effects.

We choose a Cartesian frame such that the plane walls have equations $y = \pm h$ with the direction of Ox vertically upwards and the flow is assumed to be two-dimensional in the xy-plane of the space $Oxyz$. The Boussinesq approximation is also made, in the usual notation, so that we write $\mathbf{F} = (g\beta[T - T_c], 0, 0)$, where T_c is a reference temperature and β is the volumetric-expansion coefficient.

Then we seek solutions of equations (2.1)–(2.3) subject to the boundary conditions

$$\mathbf{u} = \mathbf{0} \quad \text{on } y = \pm h \, ,$$
$$\tag{2.4}$$
$$T = T_c(1 - h^{-1}x) \quad \text{on } y = -h \, , \qquad T = T_c(1 - \mu h^{-1}x) \quad \text{on } y = h \, ,$$

where μ is a non-dimensional parameter. Note that these represent wall temperatures which decrease with increasing x. The temperature conditions in (2.4) admit of a more general form to the extent of a multiplicative factor of the term in x; this factor provides a dimensionless measure of the temperature variation.

The governing equations may be rendered dimensionless by writing

$$T = T_c(1 - T') \, , \qquad \mathbf{r} = h\mathbf{r}' \, , \qquad \mathbf{u} = \alpha h^{-1}\mathbf{u}' \, , \qquad t = h^2 \alpha^{-1} t' \, , \tag{2.5}$$

and the appropriate pressure is scaled according to $p = \rho\alpha^2 h^{-2} p'$. We also introduce a streamfunction ψ' such that $u' = \partial\psi'/\partial y'$, $v' = -\partial\psi'/\partial x'$ and $\boldsymbol{\omega}' = (0, 0, \omega')$, where $\omega' = -\nabla^2\psi'$, so that equations (2.1)–(2.3) may be written

$$\mathrm{Pr}^{-1}\{\partial(\nabla^2\psi)/\partial t + \partial(\nabla^2\psi, \psi)/\partial(x, y)\} = -\mathrm{Ra}\,\partial T/\partial y + \nabla^4\psi\,, \tag{2.6}$$

$$\partial T/\partial t + \partial(T, \psi)/\partial(x, y) = \nabla^2 T\,, \tag{2.7}$$

on omitting the dashes. In this formulation $\mathrm{Pr} = \nu/\alpha$ is the Prandtl number and $\mathrm{Ra} = g\beta T_c h^3/\nu\alpha$ is the Rayleigh number. The boundary conditions become

$$\psi = \psi_y = 0 \quad \text{on } y = \pm 1\,,$$

$$T = x \quad \text{on } y = -1\,, \qquad T = \mu x \quad \text{on } y = 1\,, \tag{2.8}$$

and we note their symmetry about the centre-plane of the channel in the case $\mu = 1$. The replacement of Ra by $-\mathrm{Ra}$ in the system (2.6)–(2.8) is equivalent to the wall temperatures increasing with increasing x, a configuration that would be expected to be stable.

Because of the special form of the boundary conditions we now seek a similarity solution of the Hiemenz type

$$\psi(x, y, t, \mathrm{Ra}, \mathrm{Pr}, \mu) = x\,f(y, t, \mathrm{Ra}, \mathrm{Pr}, \mu)\,,$$

$$T(x, y, t, \mathrm{Ra}, \mathrm{Pr}, \mu) = x\,g(y, t, \mathrm{Ra}, \mathrm{Pr}, \mu)\,. \tag{2.9}$$

It then follows that such a solution is possible if f, g satisfy

$$\mathrm{Pr}^{-1}\{f_{yyt} + f_y f_{yy} - ff_{yyy}\} = -\mathrm{Ra}\,g_y + f_{yyyy}\,,$$

$$g_t + f_y g - fg_y = g_{yy}\,, \tag{2.10}$$

and are subject to

$$f = f_y = 0 \quad \text{on } y = \pm 1\,,$$

$$g = 1 \quad \text{on } y = -1\,, \qquad g = \mu \quad \text{on } y = 1\,. \tag{2.11}$$

We may assume without loss of generality that μ lies in the range $[-1, 1]$: a simple rescaling may be applied to place μ in this range.

Equations (2.10) are, for $\mathrm{Ra} \neq 0$, coupled diffusion equations and it should be noted that other diffusion problems have been considered in which the driving mechanism is suction (or injection) at the walls $y = \pm 1$ (Zaturska, Drazin and Banks [5]) and when the flow is driven by accelerating walls (Watson, Banks, Zaturska and Drazin [6]).

The steady analogues of the equations (2.10) are obtained by writing $f(y, t, *) = F(y, *)$, $g(y, t, *) = G(y, *)$ where an asterisk represents dependence on the parameters Ra, Pr, μ; then the equations are

$$\mathrm{Pr}^{-1}(F'F'' - FF''') = -\mathrm{Ra}\,G' + F^{iv}\,,$$

$$F'G - FG' = G''\,,$$

(2.12)

with appropriate boundary conditions

$$F = F' = 0 \quad \text{on } y = \pm 1\,,$$

$$G = 1 \quad \text{on } y = -1\,, \qquad G = \mu \quad \text{on } y = 1\,.$$

(2.13)

The solution of (2.12) subject to (2.13), together with certain properties of the solution, will form the substance of this paper.

The temporal stability of such steady solutions may be investigated by writing

$$f(y, t, *) = F(y, *) + f_1(y, t, *)\,,$$

$$g(y, t, *) = G(y, *) + g_1(y, t, *)\,,$$

(2.14)

linearising equations (2.10) for small f_1, g_1 and considering normal modes with

$$f_1(y, t, *) = e^{st}\theta(y, *)\,,$$

$$g_1(y, t, *) = e^{st}\phi(y, *)\,.$$

(2.15)

We find that

$$\mathrm{Pr}^{-1}(s\theta'' - F\theta''' + F'\theta'' + F''\theta' - F'''\theta) = -\mathrm{Ra}\,\phi' + \theta^{iv}\,,$$

$$s\phi - F\phi' + F'\phi + G\theta' - G'\theta = \phi''\,,$$

(2.16)

and the boundary conditions are

$$\theta = \theta' = \phi = 0 \quad \text{on } y = \pm 1\,.$$

(2.17)

The equations (2.16) with boundary conditions (2.17) constitute an eigenproblem for the eigenfunction pair $(\theta(y), \phi(y))$ and eigenvalue s. This predicts instability of a specified steady flow F, G if $\mathrm{Re}(s) > 0$ for at least one eigenvalue.

In the numerical investigation of solutions for F, G and for θ, ϕ we have used the integrated forms of the F and θ equations. Thus

$$\mathrm{Pr}^{-1}(F'^2 - FF'') = -\mathrm{Ra}\,G + \beta_0 + F'''\,,$$

(2.18)

and

$$\mathrm{Pr}^{-1}(s\theta' - F\theta'' + 2F'\theta' - F''\theta) = -\mathrm{Ra}\,\phi + \gamma_0 + \theta'''\,,$$

(2.19)

where β_0, γ_0 are constants.

3. Some analytical results

3.1. The case $\mu = 1$

We consider first the symmetric boundary conditions corresponding to the special case $\mu = 1$. There is then a symmetric trivial solution of system (2.12) and (2.13) namely,

$$F = 0, \qquad G = 1, \tag{3.1}$$

for all Prandtl and Rayleigh numbers. For $\mathrm{Ra} < 0$, which is equivalent to the wall temperature increasing with height we expect such a solution to be stable. However, for $\mathrm{Ra} > 0$ which corresponds to wall temperature decreasing with height we anticipate that this solution will become unstable at some value of Ra. The occurrence of such an instability leads us to expect other, possibly stable, solutions.

We note from (2.16) that with the trivial steady basic flow (3.1) the exact equations for the eigenfunction pair become

$$s\,\mathrm{Pr}^{-1}\theta'' = -\mathrm{Ra}\,\phi' + \theta^{iv},$$
$$s\,\phi + \theta' = \phi'', \tag{3.2}$$

or, equivalently

$$\theta^{vi} - s(1 + \mathrm{Pr}^{-1})\theta^{iv} + (s^2\,\mathrm{Pr}^{-1} - \mathrm{Ra})\theta'' = 0. \tag{3.3}$$

For the symmetric solution (3.1) there will be both antisymmetric and symmetric modes. We use the convention that if θ' and ϕ are odd functions of y the mode is called antisymmetric, whereas if θ' and ϕ are even functions of y the mode is symmetric. For both types of modes, boundary conditions to be satisfied by (3.3) are

$$\theta = \theta' = 0 \quad \text{and} \quad s\,\mathrm{Pr}^{-1}\theta''' = \theta^{v} \quad \text{at } y = -1, \tag{3.4}$$

In what follows we shall confine attention to the special case $\mathrm{Pr} = 1$; this is not a serious restriction and we return to this point later (see Appendix).

Firstly, consider antisymmetric solutions. These are given by

$$s = -n^2\pi^2 \pm \sqrt{\mathrm{Ra}}, \qquad \theta = a\sqrt{\mathrm{Ra}}[(-1)^n - \cos n\pi y], \qquad \phi = \mp an\pi \sin n\pi y, \tag{3.5}$$

where $n = 1, 2, \ldots$ and a is a normalising factor. We note that these eigenvalues occur in complex conjugate pairs when $\mathrm{Ra} < 0$ and have real parts which are negative and independent of Ra. When $\mathrm{Ra} > 0$ there are two real eigenvalues corresponding to each value of n; these coalesce at $\mathrm{Ra} = 0$ to yield $s = -n^2\pi^2$ there.

For the symmetric modes there appears to be more than one possibility. For one we write

$$\lambda_+^2 = s + \sqrt{\mathrm{Ra}}, \qquad \lambda_-^2 = s - \sqrt{\mathrm{Ra}}. \tag{3.6}$$

Then λ_+, λ_- satisfy the relation

$$\lambda_-^3(s - \lambda_-^2)\cosh \lambda_-(\sinh \lambda_+ - \lambda_+ \cosh \lambda_+) = \lambda_+^3(s - \lambda_+^2)\cosh \lambda_+(\sinh \lambda_- - \lambda_- \cosh \lambda_-).$$

(3.7)

The information contained in equation (3.7) is not immediately obvious and it is useful, therefore, to examine special cases. In the limit as $Ra \to 0$, so that $\lambda_+ \to \lambda_-$, we find that the only solution is $s_0 = \lambda_\pm^2 = -[(2n - 1)\pi/2]^2$ for $n = 1, 2, \ldots$ where the suffix zero is used to indicate $Ra = 0$. We find that

$$\theta_0 = 0, \qquad \phi_0 = b \cos[(2n - 1)\pi y/2],$$

(3.8)

where b is a normalising factor. (These results are, of course, more readily deduced from direct solution of (3.3) with $Ra = 0$.)

Before we proceed to consider another special case of (3.7) it is opportune to discuss further the limit $Ra \to 0$. In this limit the two equations in (3.2) decouple so that the equation for θ, the perturbation in the velocity field, may be solved independently of ϕ which is related to the temperature field. From the equation for θ we find eigenvalues $s_0 = -n^2\pi^2$ (antisymmetric modes, see equation (3.5)) for $n = 1, 2, \ldots$, and $s_0 = -p^2$, where $\tan p = p$, $p > 0$ with no loss of generality (symmetric modes); the latter have corresponding eigenfunctions

$$\theta_0 = c(y \sin p - \sin py), \qquad \phi_0 = c[\tfrac{1}{2}(p \cos py - y \sin py) + p^{-1}(\cos p - \cos py)],$$

(3.9)

where c is a normalising factor, which are distinct from those of the previous paragraph (equations (3.6), (3.7)). The first three roots for p are 4.49341, 7.72525 and 10.90412 (see Abramowitz and Stegun [7]); indeed all the roots are approximated by $p = \tfrac{1}{2}(2n + 1)\pi - 2\pi^{-1}(2n + 1)^{-1}$ for $n = 1, 2, \ldots$ and we note that therefore, as n increases, the corresponding eigenvalues become very close to those corresponding to the symmetric modes of (3.6), (3.7) with $Ra = 0$ (i.e. $s_0 = -[(2n + 1)\pi/2]^2$ in this notation). Next, taking θ identically zero we find from the ϕ equation the eigenvalues $s_0 = -n^2\pi^2$ for $n = 1, 2, \ldots$ (antisymmetric modes) and $s_0 = -[(2n - 1)\pi/2]^2$ for $n = 1, 2, \ldots$, the symmetric modes of (3.6), (3.7): the corresponding eigenfunctions have already been given for these modes.

Another special case of (3.7) (or (3.2)) which is tractable is that of $s = 0$. It should be noted that the values of Ra for which $s = 0$ are of particular interest in any case since they correspond to bifurcation points of the basic solution. Moreover, in view of equations (3.2), these values of the Rayleigh number Ra will be the same for all values of the Prandtl number.

For the family of antisymmetric modes (3.5) the value when $s = 0$ corresponds to $Ra = n^4\pi^4$ for $n = 1, 2, \ldots$ which we denote by Ra_{2n-1}. Thus, the least value of Ra satisfying this property is $Ra = \pi^4 = 97.40969$. For the symmetric modes (3.6), (3.7) we have $\sqrt{Ra} = \lambda_+^2 = \lambda_-^2 = \lambda^2$, say, and (3.7) reduces to $\tanh \lambda = \tan \lambda$ with corresponding eigenfunctions

$$\theta = k(\cosh \lambda \sin \lambda y - \cos \lambda \sinh \lambda y),$$

(3.10)

$$\phi = k\lambda^{-1}(2 \cos \lambda \cosh \lambda - \cosh \lambda \cos \lambda y - \cos \lambda \cosh \lambda y),$$

where k is a normalising factor. We denote the roots of the transcendental equation by λ_n, $n = 1, 2, \ldots$. Thus the least value of Ra is found to correspond to $\lambda_1 = 3.92660$ so that Ra $= 237.72109$. These values of Ra are denoted by Ra_{2n}, $n = 1, 2, \ldots$. (The roots of $\tanh \lambda = \tan \lambda$ are well approximated by $\lambda_n = \pi(n + \frac{1}{4})$ for $n = 1, 2, \ldots$.) Direct solution of the system (3.2) with $s = 0$ for symmetric modes (θ odd, ϕ even) yields only the solution (3.10) so that $\text{Ra}_{2n} = \lambda_n^4$ gives the *only* values of the Rayleigh number at which the eigenvalues corresponding to the symmetric modes can be zero.

From the above results, supplemented by some numerical integrations which are described in the next section, we have plotted the real part of the eigenvalue, Re(s), versus Ra in Fig. 1. We have adopted the notation that $q_n^{\pm}$ denotes the antisymmetric eigenvalues and $r_n^{\pm}$ denotes the symmetric eigenvalues so that for example $q_n^+ = -n^2\pi^2 + \sqrt{\text{Ra}}$ while $q_n^- = -n^2\pi^2 - \sqrt{\text{Ra}}$. However, the first symmetric eigenvalue, which is exceptional and takes the value $-\pi^2/4$ at Ra $= 0$, is denoted by r_0. From the analytical results we anticipate that there will be a pitchfork bifurcation at Ra $=$ Ra$_1$ where Ra$_1 = 97.40909$, associated with a loss of stability of the symmetric solutions for Ra greater than this value. Similarly at Ra $=$ Ra$_2$ where Ra$_2 = 237.72109$ we expect a transcritical bifurcation to occur. Indeed, in the next section we do find that there is a pitchfork bifurcation and a transcritical bifurcation at Ra$_1$ and Ra$_2$ respectively and we further anticipate other pitchfork bifurcations and transcritical ones at Ra$_{2m-1}$ and Ra$_{2m}$ respectively for $m = 2, 3, \ldots$.

The reader may find it helpful if we summarise some of the eigenvalue results at this juncture. The values s_0 of s at Ra $= 0$, which we write $q_{0n}^{\pm}$, r_{00}, $r_{0n}^{\pm}$ for the antisymmetric and symmetric eigenvalues, are

$$q_{01}^+ = q_{01}^- = -9.870, \qquad q_{02}^+ = q_{02}^- = -39.478,$$

$$r_{00} = -2.467, \qquad r_{01}^+ = -20.197, \qquad r_{01}^- = -22.207.$$

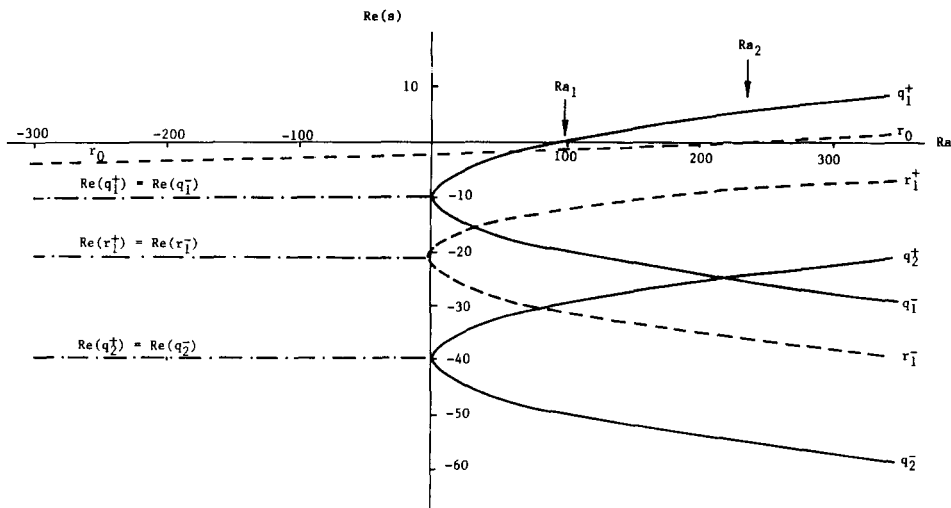Further, the values of Ra for the first six bifurcations are

Fig. 1. Some antisymmetric ($q_n^{\pm}$) and symmetric (r_0 and $r_n^{\pm}$) eigenvalues ($n = 1, 2, \ldots$) corresponding to the trivial basic solution when $\mu = 1$. The full curves represent the real antisymmetric eigenvalues, the dashed curves represent the real symmetric eigenvalues and the chain curves represent the real part of the complex eigenvalues.

$$\text{Ra}_1 = 97.41 , \qquad \text{Ra}_3 = 1558.55 , \qquad \text{Ra}_5 = 7890.14 ,$$

$$\text{Ra}_2 = 237.72 , \qquad \text{Ra}_4 = 2496.49 , \qquad \text{Ra}_6 = 10867.58 .$$

We anticipate that the odd suffices indicate supercritical pitchfork bifurcations and the even suffices indicate transcritical bifurcations.

3.2. The case $\mu \neq 1$, Ra small

When $\mu \neq 1$ there is no analytic solution of (2.12) subject to (2.13) for all Ra. For small Rayleigh number the regular solution is unique for each value of μ: we write

$$G(y, *) = G_0(y, \mu) + \text{Ra}\, G_1(y, \mu) + \cdots ,$$

$$F(y, *) = \text{Ra}\, F_1(y, \mu) + \cdots , \quad \text{as } \text{Ra} \to 0 , \tag{3.11}$$

and, on solving at successive approximations, we find

$$G_0(y, \mu) = \tfrac{1}{2}(1 - y) + \tfrac{1}{2}\mu(1 + y) ,$$

$$F_1(y, \mu) = - \frac{1}{48} (1 - \mu)(1 - y^2)^2 , \tag{3.12}$$

and

$$G_1(y, \mu) = \frac{(1 - \mu)^2}{2880} (1 - y^2)(17 + 2y^2 - 3y^4) - \frac{(1 - \mu^2)}{1440} y(7 - 3y^2)(1 - y^2) .$$

We proceed similarly for the eigenfunctions (θ, ϕ) and find that the leading order terms (θ_0, ϕ_0) consist of three families: there are modes that are antisymmetric, symmetric and asymmetric. They are

(i) antisymmetric modes:

$$s_0 = -n^2\pi^2 , \qquad \theta_0 = 0 , \qquad \phi_0 = a \sin n\pi y , \tag{3.13}$$

where $n = 1, 2, \ldots$ and a is a normalising factor.

(ii) symmetric modes:

$$s_0 = -[(2n - 1)\pi/2]^2 , \qquad \theta_0 = 0 , \qquad \phi_0 = b \cos[(2n - 1)\pi y/2] , \tag{3.14}$$

where $n = 1, 2, \ldots$ and b is a normalising factor.

(iii) asymmetric modes:

$$s_0 = -p^2 , \qquad \theta_0 = c(y \sin p - \sin py)$$

$$\phi_0 = \frac{c}{8} \{(1 + \mu)[4p^{-1}(\cos p - \cos py) + 2(p \cos py - y \sin py)] \tag{3.15}$$

$$+ (1 - \mu)[(y^2 - 1) \sin py + 3p^{-2}(py \cos py - \sin py)]\} ,$$

where $\tan p = p$, $p > 0$, and c is a normalising factor. We note that when $\mu = 1$ (3.15) reduces to (3.9).

It is clear, since $s < 0$ for each of these modes, that the basic solution as given by the terms of $O(1)$ in (3.11) is stable.

4. Numerical results

It has already been noted that there are certain simplifications in the analysis if the Prandtl number is one and we continue with this special value in this section, although we also note that there is no great loss of generality in so doing (see Appendix).

As we have seen in §3 some of the eigenvalues corresponding to the trivial basic flow are known analytically, some for special values of the Rayleigh number and some for all Rayleigh numbers. We begin this section by presenting numerical results for other eigenvalues: in particular we have obtained the eigenvalues that are continued from those that at $Ra = 0$ take the values $-\pi^2/4$, $-p^2$ and $-9\pi^2/4$ where p is the first positive root of $\tan p = p$. This has been done by using the shooting method (as have all the other numerical integrations of this section) to solve the eigenvalue problem as defined by (3.2) and (3.4). The results are shown in Fig. 1 where we have plotted $\mathrm{Re}(s)$ versus Ra. We have only plotted the most significant eigenvalues in the range $-300 \leqslant Ra \leqslant 300$, to give a flavour of the structure; as mentioned earlier, the important results are those values of the Rayleigh number where $\mathrm{Re}(s) = 0$ (which are summarised near the end of §3.1), because we anticipate the possibility of bifurcations at such points. Since there exists an eigenvalue $s > 0$ for $Ra > 97.4091$, then the trivial solution is unstable for $Ra > Ra_1$. It is of interest to note that the symmetric eigenvalues, which pass through the points $-9\pi^2/4(= -22.2066)$ and -20.1969 at $Ra = 0$, coalesce at $Ra = -1.143$ so that for $Ra < -1.143$ the eigenvalues are complex.

As the Rayleigh number increases we recall that the first bifurcation we meet is at $Ra = Ra_1 = \pi^4 = 97.4091$ in the neighbourhood of which we anticipate asymmetric solutions – even though the boundary conditions are symmetric. We have integrated the system of equations defined by (2.12) subject to the symmetric boundary conditions (2.13) with $\mu = 1$ and we have indeed found asymmetric solutions in the neighbourhood of $Ra = Ra_1$, and have continued with the asymmetric branch as Ra increases. We note incidentally that the pitchfork bifurcation is supercritical and that the analytic structure of the solution in the vicinity of $Ra = Ra_1$ is given in §5.

To appreciate these results it is convenient to show the variation of a norm or property of the solution in terms of Ra. In this paper we have chosen to use the variation of $G'(-1)$, which is related to the heat transfer, and of $F''(-1)$, which is related to the skin-friction, at the wall $y = -1$. These results are shown in Figs 2 and 3: it should be noted that the trivial solution, $G \equiv 1$, $F \equiv 0$, is represented by the Ra-axis in both figures. Referring to Figs 2 and 3 we see that the pair of asymmetric solutions that arise at $Ra = Ra_1$ coalesce at $Ra = Ra_{1,1} = 125.36$ to form a single non-trivial symmetric solution there – in other words, a subcritical pitchfork bifurcation is formed at $Ra_{1,1}$. Subsequent bifurcations from this non-trivial symmetric solution branch will be labelled $Ra_{1,2}$, $Ra_{1,3}$, etc. We have continued with the tabulation of the non-trivial symmetric solution for both $Ra \gtrless Ra_{1,1}$. Firstly, for $Ra < Ra_{1,1}$ we find as $Ra \downarrow 0$ that $G'(-1) \to \infty$ so that there is blow-up in the heat transfer: indeed at $Ra = 0$ we obtain $Ra\, G'(-1) = 205.80$ and $F''(-1) = 25.27$. (These results are
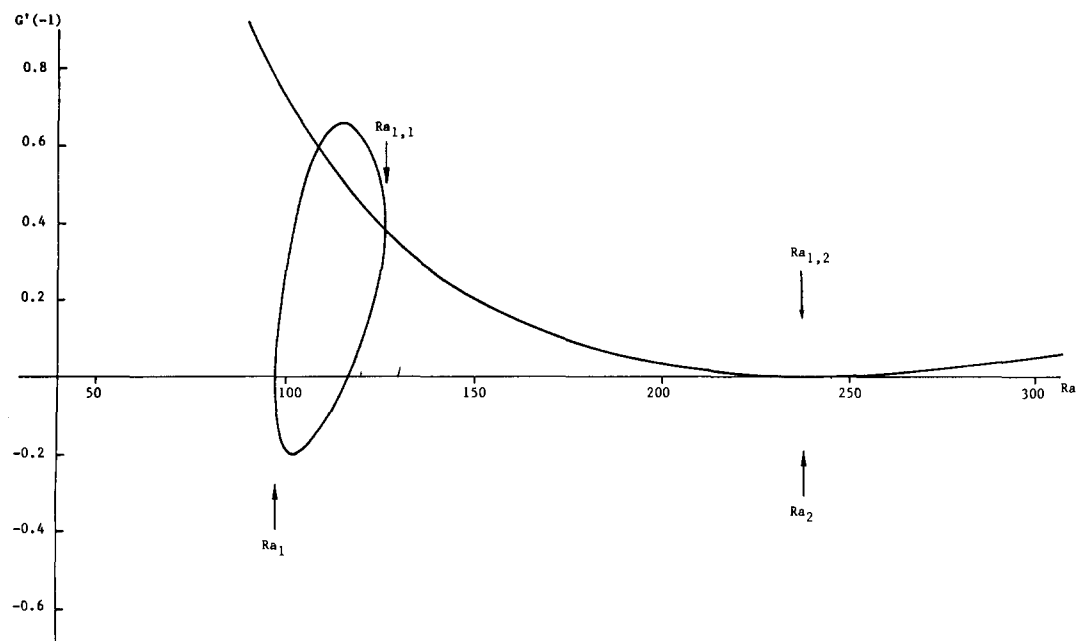
Fig. 2. Values of $G'(-1)$ versus Ra, showing two pitchfork bifurcations (at Ra_1 and $Ra_{1,1}$) and one transcritical bifurcation (at Ra_2).

shown graphically in Figs 4 and 5). It is sufficient to note at this stage that for $Ra < Ra_{1,1}$ no further bifurcations were found on this non-trivial symmetric branch. Secondly, for $Ra > Ra_{1,1}$ the continuation of the solution branch is found to form part of the transcritical bifurcation at $Ra = Ra_2 = 237.72$ and referred to in §5. We note incidentally that in terms of the state variable $F''(-1)$ the solution branches are of typical transcritical type at $Ra = Ra_2$
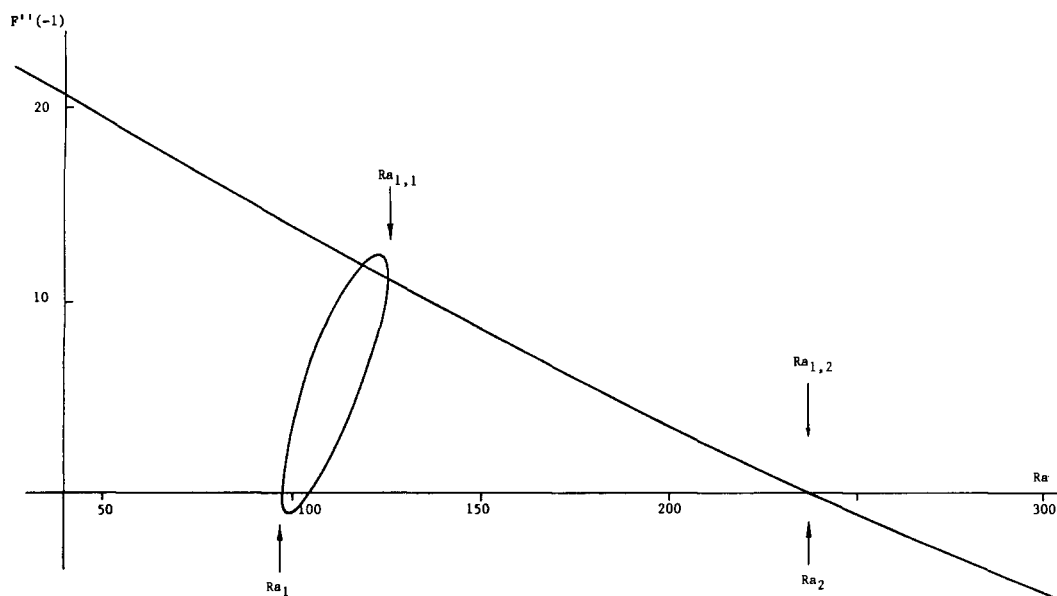

Fig. 3. Values of $F''(-1)$ versus Ra, showing two pitchfork bifurcations (at Ra_1 and $Ra_{1,1}$) and one transcritical bifurcation (at Ra_2).
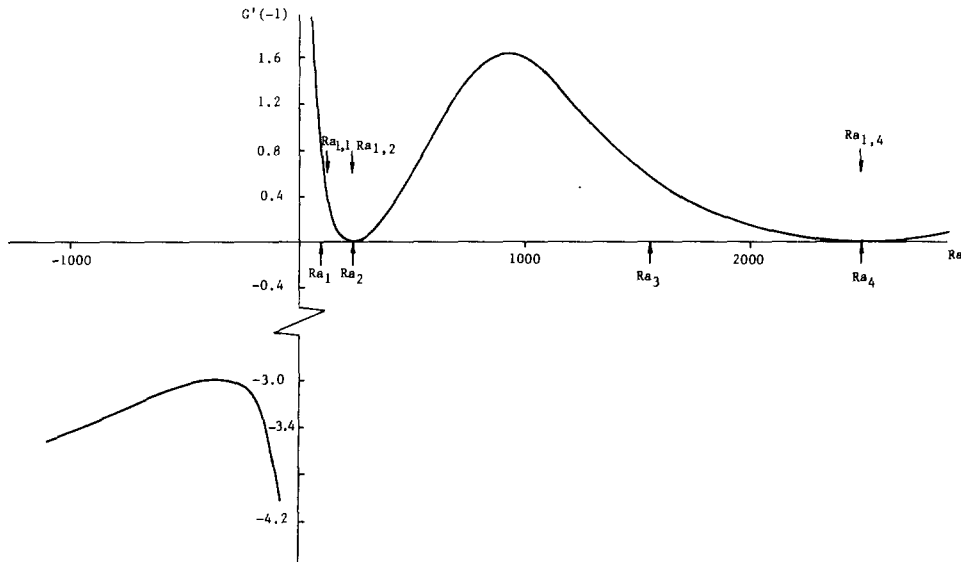
Fig. 4. Values of $G'(-1)$ versus Ra corresponding to the non-trivial symmetric solution. The values of Ra at which bifurcations occur are indicated.

whereas this is not so with the state variable $G'(-1)$: this distinction is also noted in the analytical structure of the local analysis of §5.

We have continued with the integrations on the non-trivial symmetric branch over the range $-500 \leqslant \text{Ra} \leqslant 3000$ and most of these results are shown in Figs 4 and 5. In order to help the reader we have marked with a vertical arrow below the Ra-axis, those values of Ra, i.e. Ra_n, at which there is a bifurcation point in the trivial solution; also we have used downward
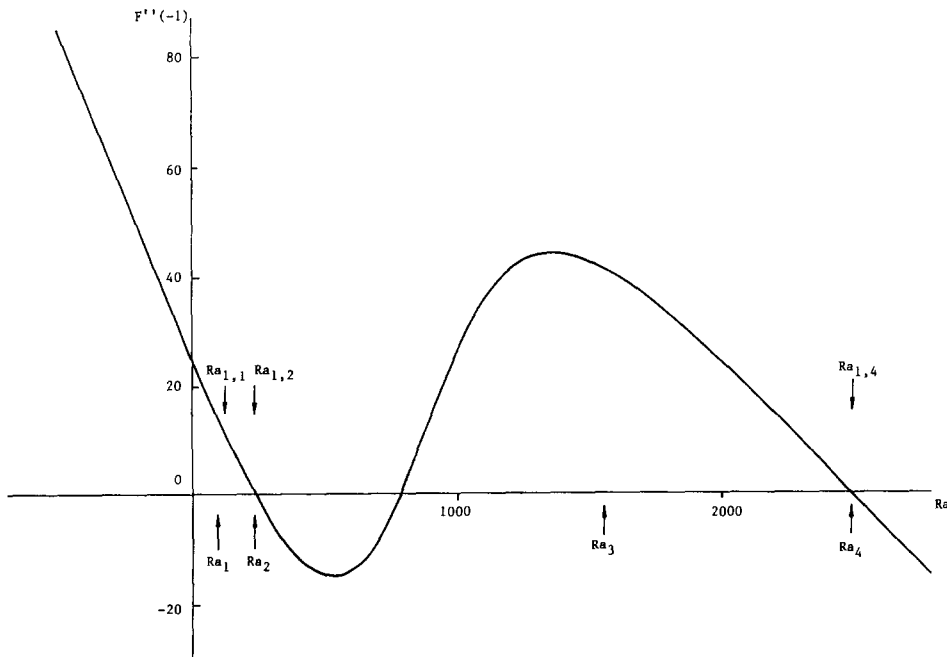

Fig. 5. Values of $F''(-1)$ versus Ra corresponding to the non-trivial symmetric solution. The values of Ra at which bifurcations occur are indicated.

pointing arrows above the Ra-axis to indicate the values $Ra_{1,n}$. Note that Ra_2 coincides with $Ra_{1,2}$ because the non-trivial solution branch intersects the trivial solution branch. It will be noted that we have indicated the known bifurcation points $Ra_{1,1}$, $Ra_{1,2}$, $Ra_{1,4}$ but not $Ra_{1,3}$; we have not found $Ra_{1,3}$ although we anticipate such a subcritical pitchfork bifurcation point to exist in the same way that we assume that asymmetric solutions occur for Ra near to but greater than Ra_3. In short, we assume that the topology of the solution branches in the region $Ra_1 \leqslant Ra \leqslant Ra_2$ is repeated by the solution branches in $Ra_3 \leqslant Ra \leqslant Ra_4$. We note that although the solutions in this region correspond to unstable flows which are physically non-realisable, it is possible that such solutions may be significant in the interpretation of the possible unsteady solutions of the coupled diffusion equations as defined by (2.10) and (2.11).

In order to help the reader visualise the flow and temperature régimes, we present in Fig. 6, the velocity profiles and the corresponding temperature profiles at representative values of Ra: these values were chosen by reference to Fig. 2. We show at $Ra = 106$ ($>Ra_1$) and $Ra = 120$ ($<Ra_{1,1}$) the steady asymmetric solutions; at $Ra = 130$ ($>Ra_{1,1}$) there are no steady asymmetric solutions and we present the non-trivial steady symmetric solution.

We have determined a number of eigenvalues corresponding to the asymmetric and the non-trivial symmetric solutions discussed above; we show some of these in Fig. 7 where we have plotted $Re(s)$ versus Ra but have confined attention to a relatively small range of Ra which includes the asymmetric solutions in $Ra_1 < Ra < Ra_{1,1}$. We notice that, after the first zero in an eigenvalue at Ra_1, the continuation of the first two eigenvalues along the asymmetric branch leads to a coalescing of the eigenvalues at $Ra \approx 100.7$; beyond this value of Ra the eigenvalues become complex with $Re(s) < 0$ at first so that the flow remains stable. At $Ra = 112.65$ the real part of these complex eigenvalues vanish and we infer the existence of a Hopf bifurcation – we denote this value by Ra_H.

For $Ra > Ra_H$ we anticipate the existence of periodic solutions. As Ra increases beyond Ra_H the real part of the complex eigenvalues increases and at $Ra = 122.7$ we note the appearance of two real eigenvalues; both are positive corresponding to unstable modes. One of these eigenvalues vanishes at $Ra = Ra_{1,1}$ where $Ra_{1,1} = 125.36$, which indicates the
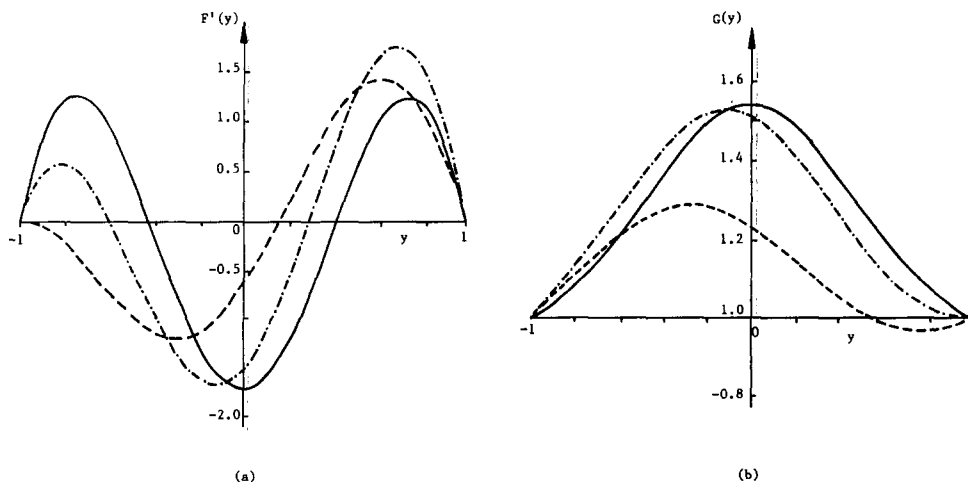

(a)   (b)

Fig. 6. (a) Velocity profiles and (b) temperature profiles at representative values of the Rayleigh number. The dashed curves correspond to the asymmetric flow at $Ra = 106$ and the chain curves to the asymmetric flow at $Ra = 120$. The full curve corresponds to the non-trivial symmetric flow at $Ra = 130$.
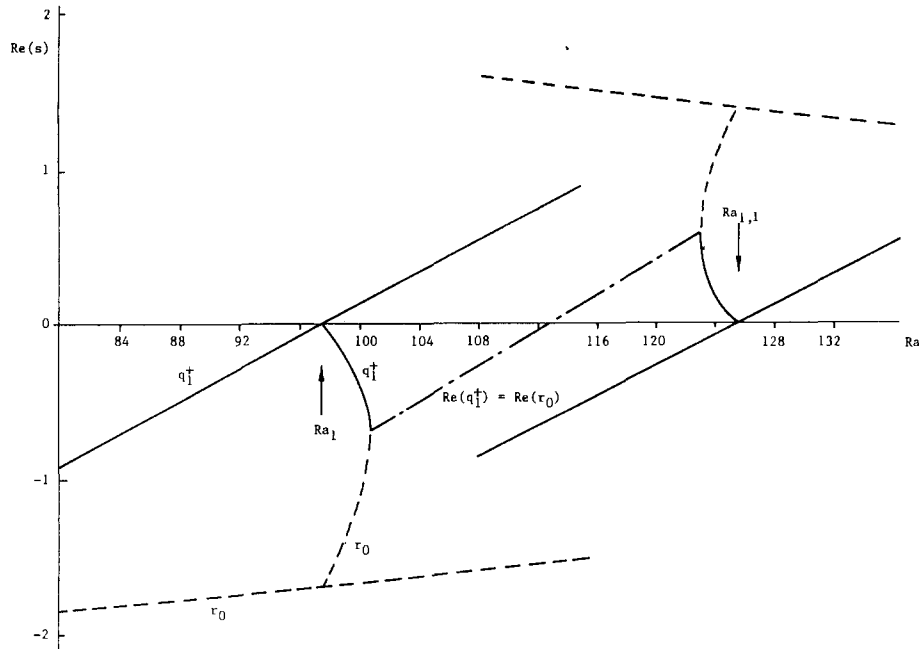
Fig. 7. Some eigenvalues corresponding to the trivial symmetric, the asymmetric and to the non-trivial symmetric basic solutions. The full curves represent the real 'antisymmetric' modes (q_1^{+}), the dashed curves represent the real 'symmetric' modes (r_0) and the chain curve represents the real part of the complex eigenvalues.

appearance of the subcritical pitchfork bifurcation resulting in the existence of the non-trivial symmetric branch. We have found the continuation of these eigenvalues on the non-trivial symmetric branch for a wide range of values of Ra but we have only plotted those in the range $108 \leqslant \mathrm{Ra} \leqslant 134$. However, from our results we find that the eigenvalue that passes through 1.4 at $\mathrm{Ra} = \mathrm{Ra}_{1,2}$ continues to decrease as Ra increases, and vanishes at $\mathrm{Ra} = \mathrm{Ra}_{1,4} = \mathrm{Ra}_4$ corresponding to the second transcritical bifurcation point. From this it might appear that, for $\mathrm{Ra} > \mathrm{Ra}_4$, there is only one unstable component of the set of eigenfunctions but it should be remembered that we have not determined the higher order modes. In Fig. 7 we have used a dashed line to indicate eigenvalues corresponding to symmetric modes and a solid line to indicate eigenvalues for antisymmetric modes, and we note the form of the real eigenvalues for $\mathrm{Ra} > 122.7$; the same scheme for distinguishing the modes is used in continuing from those corresponding to a symmetric basic solution to those where the basic solution is asymmetric, although these latter modes are themselves no longer symmetric or antisymmetric.

Finally, in this section, we consider the effect of $\mu \neq 1$, that is, the effect of asymmetry in the boundary conditions. As noted earlier, it is sufficient to restrict attention to the range $-1 \leqslant \mu \leqslant 1$. To illustrate the ideas, we show in Fig. 8 the effect of a perturbation in the symmetric conditions: we examine the effect of assuming $\mu = 0.9999$ and note the change from a pitchfork bifurcation at $\mu = 1$ with $\mathrm{Ra} = \mathrm{Ra}_1$ to a single turning point. It is opportune, at this stage, to introduce some notation. On breaking the symmetry we label the solution curve that continues from $\mathrm{Ra} = 0$ by P (primary), and the branch that includes the turning point we denote by S (secondary): S_1 corresponds to those solutions that have evolved from the trivial solution and S_2 to those that have evolved from the asymmetric solutions. This notation can be extended as μ varies further from unity and to all Ra: we continue to denote
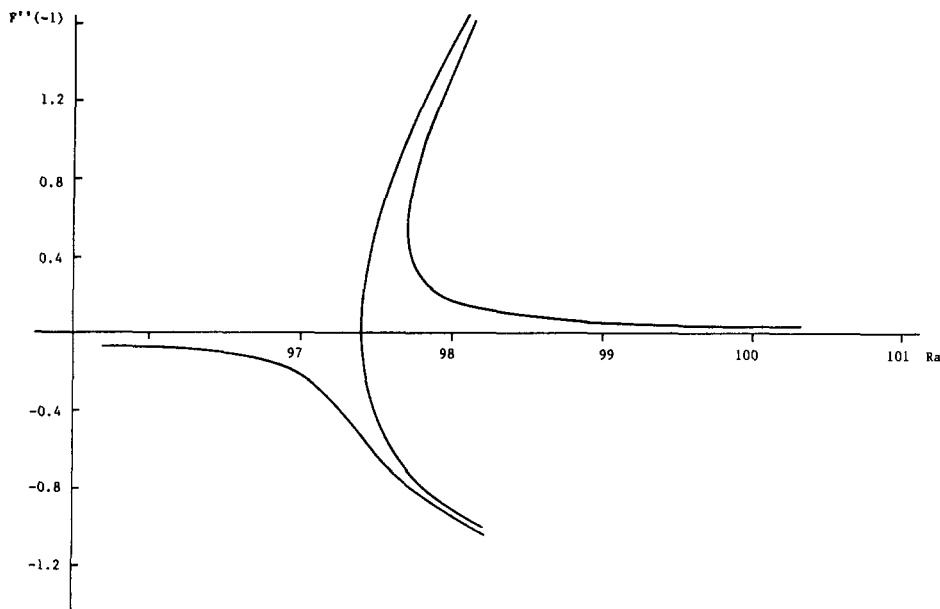
Fig. 8. Values of $F''(-1)$ versus Ra for $\mu = 1$ and $\mu = 0.9999$ showing the unfolding of the pitchfork bifurcation.

the solution curve that continues from Ra = 0 by P but, as it too develops a turning point, the branch that has evolved from the trivial solution is denoted by P_1 and the other branch by P_2. We also continue to use S_1 to correspond to those secondary solutions that have evolved from the trivial symmetric solution but S_2 represents solutions which have evolved from the asymmetric solutions and from the non-trivial symmetric solutions. Symmetry breaking occurs at the other bifurcations for a change in μ resulting in turning points, and we have calculated the locus of these turning points as μ varies. To do this we solve for the basic flow and eigenfunctions concurrently with $s = 0$. The locus of the turning point that originates at Ra = $Ra_{1,2}$ is shown in Fig. 9: we see that as μ decreases so the turning point moves monotonically towards the μ-axis until at $\mu = -1$ it is at Ra = 50.29. In view of the symmetry of the solution about Ra = 0 for $\mu = -1$ we note that there is a turning point at Ra = -50.29 for this value of μ. We have also determined the locus of the turning point starting at $\mu = -1$, Ra = -50.29 with μ increasing, and, as will be noted in Fig. 9, the value of Ra at the turning point appears to tend to minus infinity as $\mu \uparrow 0$: we find, for example, that the turning point occurs at Ra = -1226.56 when $\mu = 0.009$.

In Fig. 10 we also give the loci of the other turning points and we see that the one emanating at Ra = Ra_1 and *one* of those that emanates from Ra = Ra_2 are connected: the consequences of this joining are discussed later. Note also that the value of Ra at the *second* turning point, that emanates from Ra = Ra_2, increases as μ decreases: at $\mu = 0.684$ the turning point is at Ra = 758.00; the consequences of this behaviour are also discussed later. We have plotted the loci of the turning points just referred to in Fig. 11 to show the general behaviour.

With $\mu = 1$ there is, as mentioned earlier, a Hopf bifurcation at Ra = Ra_H where $Ra_H = 112.65$, when the flow is asymmetric. In the range $Ra_1 < Ra < Ra_2$, in which asymmetric solutions exist, it is clear that for each value of the Rayleigh number, Ra, there are two steady solutions: one the mirror image (in the channel's mid-plane) of the other. Similarly there are two Hopf bifurcation points, one on each solution branch. To find the loci
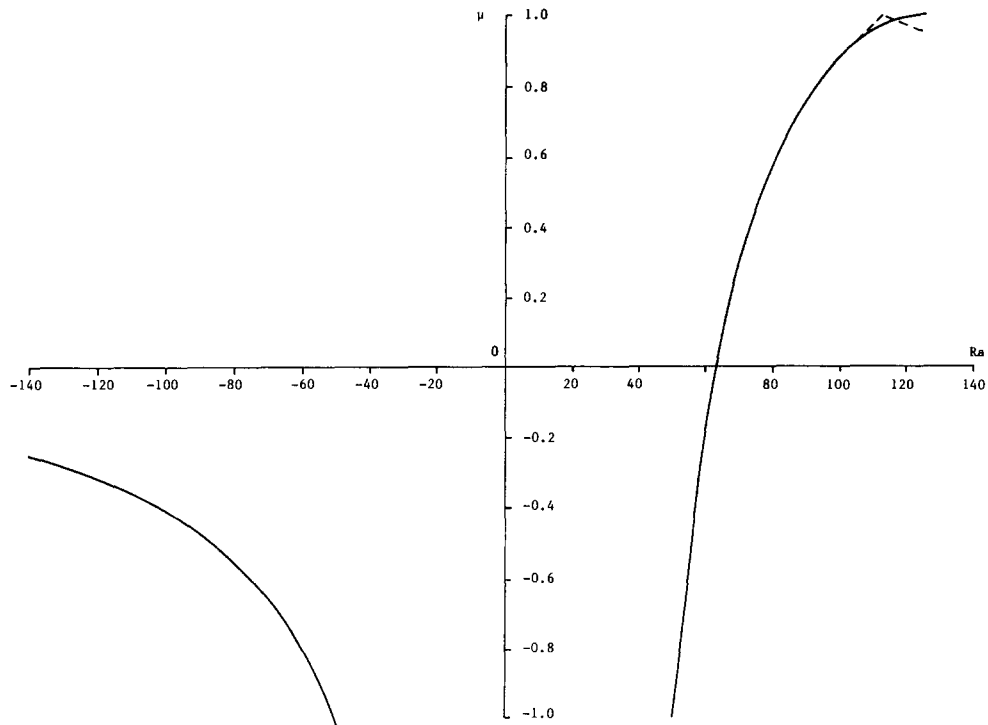
Fig. 9. Locus of the turning point that originates at $Ra = Ra_{1,2}$, $\mu = 1$, for various values of μ, shown as a full curve. The dashed lines represent the loci of the Hopf bifurcations.
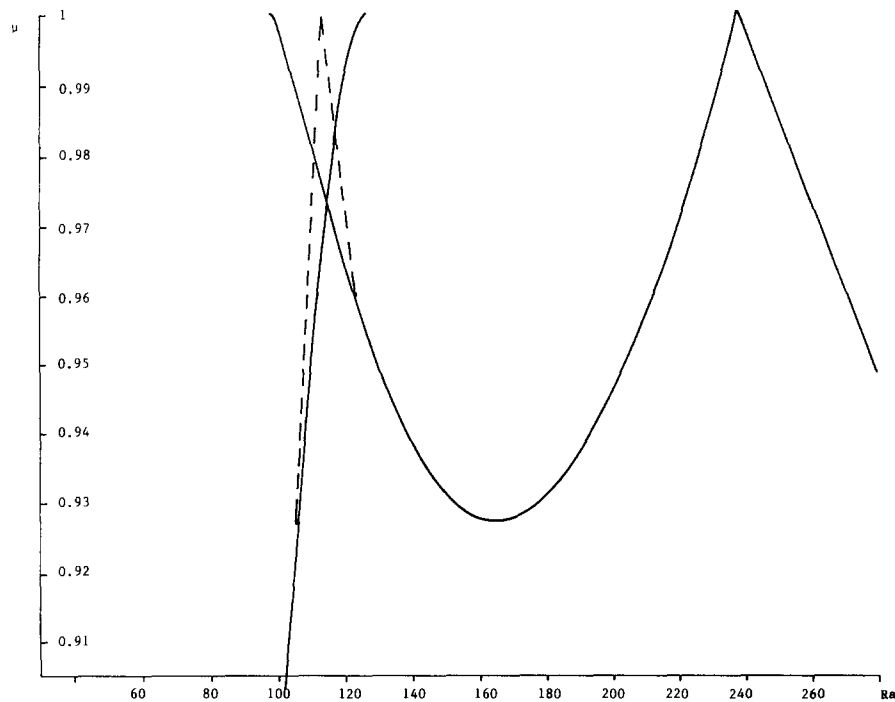

Fig. 10. Loci of the turning points originating at $Ra = Ra_1$ and at $Ra = Ra_2$ when $\mu = 1$, together with the loci of the Hopf bifurcations originating at $Ra = Ra_H$ when $\mu = 1$, for various values of μ.
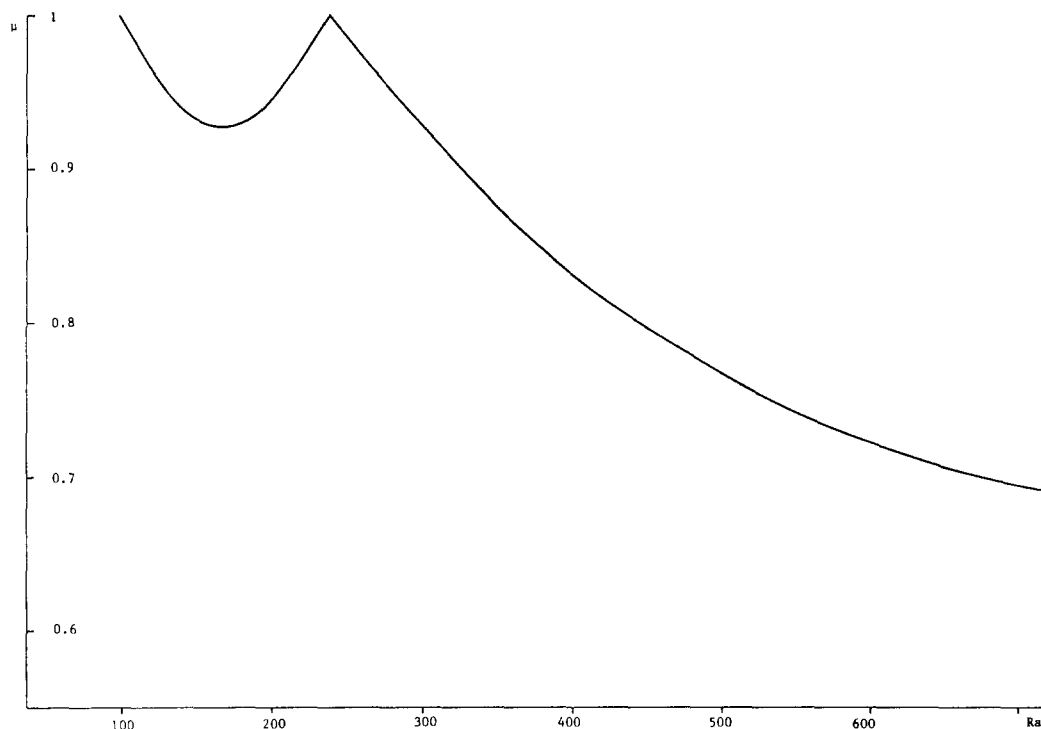
Fig. 11. Loci of the turning points originating at Ra = Ra$_1$ and at Ra = Ra$_2$ when μ = 1, for various values of μ.

of these Hopf bifurcation points as μ varies we have solved for the basic flow and complex eigenfunctions concurrently with Re(s) = 0. We show the loci of these bifurcation points in Fig. 10 and we note that in both cases the Hopf bifurcation points approach the turning point loci as μ decreases from its value of unity corresponding to symmetry. It may help if we show, by means of sketches in Fig. 12, the behaviour of the eigenvalues as μ decreases from 1− until the Hopf bifurcation coincides with the turning point. We anticipate that the point at which the loci of the Hopf bifurcation points and of the turning points coincide is a Takens–Bogdanov bifurcation (see Guckenheimer and Holmes [8]). No special computations were carried out in the vicinity of this point and we merely refer the interested reader to the work of Watson, Banks, Zaturska and Drazin [9] for more information.

We now return to the consequences of the turning-point loci. These enable us to sketch the form of the solution curves quite readily. In Fig. 13 we give sketches of the solution branches corresponding to $F''(-1)$ for various values of μ. We note that, for $0 < 1 - \mu \ll 1$, at least one isola exists with the possibility of others at higher Rayleigh numbers. From Fig. 11 we see that as $\mu \downarrow 0.927$ the isola shrinks to a single point and that for $\mu < 0.927$ this branch of solutions ceases to exist. In making these sketches we have not only used the results of the turning-point loci but the blow-up results quoted earlier, viz. Ra $G'(-1) = 205.80$ and $F''(-1) = 25.27$: these results are independent of μ of course.

5. Local bifurcation theory

We next consider perturbations of a solution of (2.12) subject to (2.13) in order to investigate the bifurcations that occur. Suppose that $F = F_0$, $G = G_0$ is a solution when
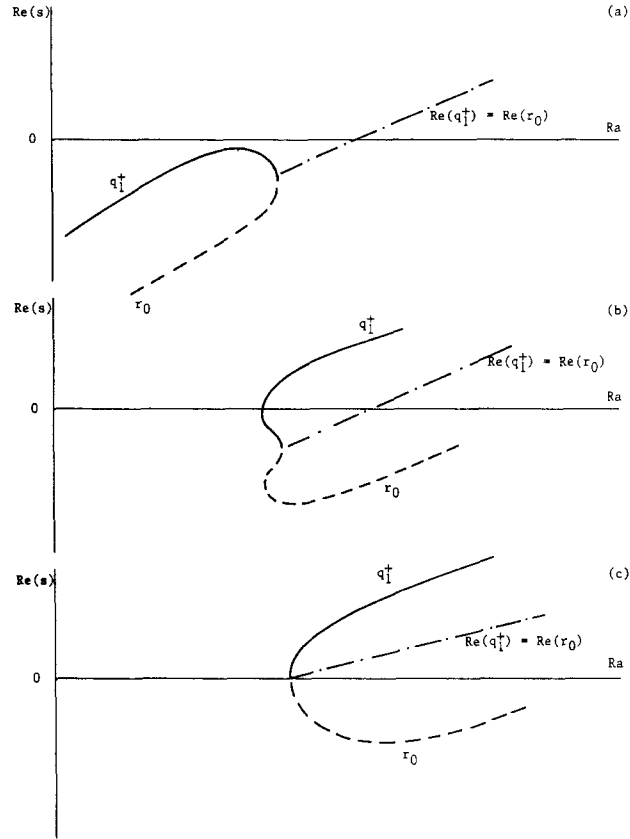
Fig. 12. Qualitative sketches of the behaviour of some eigenvalues for various μ. (a) $\mu = 1-$, (b) $\mu \approx 0.98$, (c) $\mu \approx 0.96$.

$\mathrm{Ra} = \mathrm{Ra}_c$; we continue to restrict our analysis to the case $\mathrm{Pr} = 1$ although recognising that any change in Prandtl number will result in a change of degree rather than of character. We perturb this solution for small $\varepsilon = \mathrm{Ra} - \mathrm{Ra}_c$, anticipating that a series in powers of ε is appropriate at a regular point but in powers of $\varepsilon^{1/2}$ at a turning point or at a pitchfork bifurcation. Accordingly we assume the expansions

$$F = F_0 + \varepsilon^{1/2} F_{1/2} + \varepsilon F_1 + \cdots ,$$

$$G = G_0 + \varepsilon^{1/2} G_{1/2} + \varepsilon G_1 + \cdots ,$$

(5.1)

and substitute them into the steady equations (2.12). Equating coefficients of ε^0 determines F_0, G_0.

Next we equate coefficients of $\varepsilon^{1/2}$ and find that

$$L \begin{pmatrix} F_{1/2} \\ G_{1/2} \end{pmatrix} = 0 ,$$

(5.2)

where the operator L is defined by

$$L \begin{pmatrix} u \\ v \end{pmatrix} = \begin{pmatrix} u^{iv} + F_0 u''' - F_0' u'' - F_0'' u' + F_0''' u - \mathrm{Ra}_c v' \\ v'' + F_0 v' - F_0' v - G_0 u' + G_0' u \end{pmatrix}$$
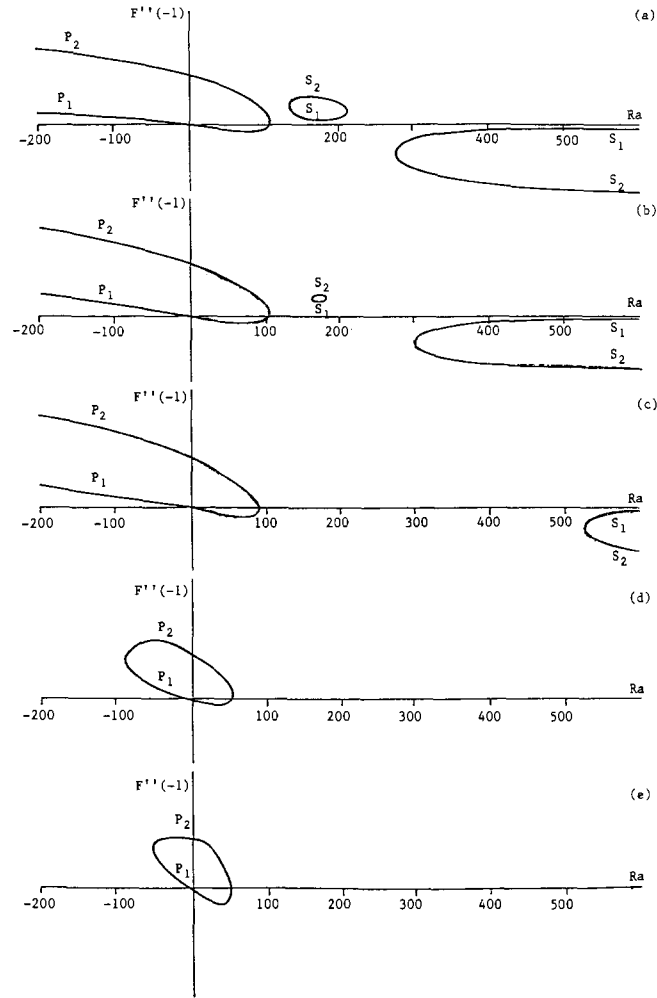
(5.3)

Fig. 13. Qualitative sketches of the solution branches for $F''(-1)$ versus Ra for various values of μ, showing the presence of an isola. (a) $\mu \approx 0.95$, (b) $\mu \approx 0.928$, (c) $\mu \approx 0.75$, (d) $\mu \approx -0.5$, (e) $\mu = -1$.

for all well-behaved functions u, v. The boundary conditions are

$$F_{1/2}(\pm 1) = F'_{1/2}(\pm 1) = G_{1/2}(\pm 1) = 0 \,. \tag{5.4}$$

Comparison of the system (5.2), (5.4) with (2.16), (2.17) leads to the conclusion that at a regular point, where $s \neq 0$ for all eigenvalues, the only possible solution is the trivial one $F_{1/2} = G_{1/2} = 0$. We therefore assume that $s = 0$. Then the system (5.2), (5.4) has solution

$$\begin{pmatrix} F_{1/2} \\ G_{1/2} \end{pmatrix} = A \begin{pmatrix} \theta \\ \phi \end{pmatrix} \,, \tag{5.5}$$

where A is a constant which is arbitrary at this stage but will be determined later.

Proceeding to terms in ε^1, substituting for $F_{1/2}$, $G_{1/2}$, and applying a solvability condition we find at length that

$$I_1 + A^2 I_2 = 0 \,, \tag{5.6}$$

where

$$I_1 = - \int_{-1}^{1} \theta^+ G_0' \, dy \, , \tag{5.7}$$

$$I_2 = \int_{-1}^{1} [\theta^+ (\theta' \theta'' - \theta \theta''') + \phi^+ (\theta' \phi - \theta \phi')] \, dy \, , \tag{5.8}$$

and the functions θ^+, ϕ^+ satisfy the adjoint equation

$$L^+ \begin{pmatrix} \theta^+ \\ \phi^+ \end{pmatrix} = \begin{pmatrix} \theta^{+iv} - (F_0 \theta^{+'''} + 4F_0' \theta^{+''} + 4F_0'' \theta^{+'}) + G_0 \phi^{+'} + 2G_0' \phi^+ \\ \phi^{+''} - (F_0 \phi^{+'} + 2F_0' \phi^+) - Ra_c \theta^{+'} \end{pmatrix} = 0 \tag{5.9}$$

subject to $\theta^+(\pm 1) = \theta^{+'}(\pm 1) = \phi^+(\pm 1) = 0$. We note that non-trivial θ^+, ϕ^+ exist because $s = 0$. Various cases arise depending on the vanishing or otherwise of the integrals and we discuss these below.

(i) $s = 0$, $I_1 \neq 0$, $I_2 \neq 0$. Under these circumstances, F, G each have a power series in $\pm (\varepsilon \, \mathrm{sgn} \, A^2)^{1/2}$ with two solutions for Ra near Ra_c if $Ra > Ra_c$ and none if $Ra < Ra_c$ when $A^2 > 0$, and two solutions if $Ra < Ra_c$ and none if $Ra > Ra_c$ when $A^2 < 0$ respectively. The bifurcation is a turning point and $A^2 = -I_1/I_2$.

(ii) $s = 0$, $I_1 = 0$, $I_2 \neq 0$. In this case $A = 0$ and F, G have power series in ε with two solutions for Ra near Ra_c (and one for $Ra = Ra_c$) i.e. a transcritical bifurcation.

(iii) $s = 0$, $I_1 = 0$, $I_2 = 0$. Then A is indeterminate at this stage but we formally write

$$F_1 = A^2 H_1 + H_2 \, , \qquad G_1 = A^2 K_1 \, , \tag{5.10}$$

where

$$L \begin{pmatrix} H_1 \\ K_1 \end{pmatrix} = \begin{pmatrix} \theta' \theta'' - \theta \theta''' \\ \theta' \phi - \theta \phi' \end{pmatrix} , \tag{5.11}$$

$$L \begin{pmatrix} H_2 \\ 0 \end{pmatrix} = \begin{pmatrix} -G_0' \\ 0 \end{pmatrix} , \tag{5.12}$$

and $H_1(\pm 1) = H_1'(\pm 1) = H_2(\pm 1) = H_2'(\pm 1) = K_1(\pm 1) = 0$. Proceeding to terms in $\varepsilon^{3/2}$ and applying the solvability condition we find that $A = 0$, or

$$A^2 = -I_3/I_4 \, , \tag{5.13}$$

where

$$I_3 = \int_{-1}^{1} [\theta^+ (-H_2 \theta''' + H_2' \theta'' + H_2'' \theta - H_2''' \theta - \phi') + \phi^+ (-H_2 \phi' + H_2' \phi)] \, dy \, , \tag{5.14}$$

$$I_4 = \int_{-1}^{1} [\theta^+ (-H_1 \theta''' + H_1' \theta'' + H_1'' \theta' - H_1''' \theta) + \phi^+ (-H_1 \phi' + H_1' \phi + K_1 \theta' - K_1' \theta)] \, dy \, . \tag{5.15}$$

If F_0, G_0 correspond to a symmetric flow (i.e. F_0 is an even function of y and G_0 an odd one) then the root $A = 0$ corresponds to a continuation of the same flow and the other two roots to asymmetric flows; F, G have expansions in powers of $\pm|\varepsilon|^{1/2}$ so that there are three solutions for Ra near Ra_c if either $\text{Ra} > \text{Ra}_c$ or $\text{Ra} < \text{Ra}_c$ and one if $\text{Ra} < \text{Ra}_c$ or $\text{Ra} > \text{Ra}_c$ respectively. This pitchfork bifurcation will in general arise if F_0, ϕ, ϕ^+ are odd functions of y and θ, θ^+ are even ones, i.e. when $s = 0$ for an antisymmetric mode. We would similarly expect turning point bifurcations (case (i)) when $s = 0$ for a symmetric mode.

Further progress may be made analytically when the basic flow is the trivial one $F_0 = 0$, $G_0 = 1$, for then the eigenfunctions are known at values of Ra when $s = 0$, and the integrals are considerably simplified. At the first bifurcation point where $\text{Ra} = \text{Ra}_1 = \pi^4$ we find that $I_1 = I_2 = 0$, i.e. case (iii). We have evaluated the integrals I_3, I_4 for the corresponding antisymmetric mode given by (3.5) when $n = 1$ and in this case we find $A^2 = -(3.9\pi^2)^{-1}$. This analytic result predicts that

$$F''(-1) = -1.590807(\text{Ra} - \text{Ra}_1)^{1/2} + O(\text{Ra} - \text{Ra}_1)$$

and

$$G'(-1) = 0.161118(\text{Ra} - \text{Ra}_1)^{1/2} + O(\text{Ra} - \text{Ra}_1) \quad \text{as Ra} \to \text{Ra}_1$$

so that at $\text{Ra} = 97.40925$, $F''(-1) = -0.020057$ and $G'(-1) = 0.002032$ to first order; this shows excellent agreement with the corresponding results from direct numerical integration, viz. -0.019937 and 0.002032 respectively. The contributions from the terms of order of magnitude $(\text{Ra} - \text{Ra}_1)$ in the expansions may also be readily evaluated in this case.

When $s = 0$ corresponds to symmetric modes and trivial basic solution, $I_1 = 0$ and $I_2 \neq 0$ so that case (ii) applies and thus $A = 0$, and the expansion is in powers of ε. Then the solution

$$\binom{F_1}{G_1} = B \binom{\theta}{\phi} \tag{5.16}$$

is obtained on equating coefficients of ε^1; the constant B is arbitrary at this stage. We next equate coefficients of ε^2, substitute for F_1 and G_1, and apply a solvability condition to find that either $B = 0$ or

$$B = I_5/I_6 , \tag{5.17}$$

where

$$I_5 = \int_{-1}^{1} \theta^+ \phi \, dy , \tag{5.18}$$

$$I_6 = \int_{-1}^{1} [\theta^+ (\theta'\theta'' - \theta\theta''') + \phi^+ (\theta'\phi - \theta\phi')] \, dy . \tag{5.19}$$

The root $B = 0$ corresponds to the continuation of the trivial solution and the other root to a symmetric flow. We have evaluated the integrals I_5, I_6 analytically for the symmetric modes given by (3.10). We find that $\theta^+ = \theta$, $\phi^+ = -\lambda^4 \phi$ and $B = 5[\lambda^2 \cosh \lambda(30\lambda \cos \lambda - 8 \sin \lambda)]^{-1}$ so that when $\lambda = 3.92660$ (i.e. $\text{Ra}_c = \text{Ra}_2 = 237.72109$), $B = -1.6452 \times 10^{-4}$. This analytical

result predicts that $F''(-1) = 0.90999(\text{Ra} - \text{Ra}_2) + O((\text{Ra} - \text{Ra}_2)^2)$ as $\text{Ra} \rightarrow \text{Ra}_2$ so that at $\text{Ra} = 238$, $F''(-1) = -0.0256$ to first order; this shows excellent agreement with $F''(-1) = -0.0258$, the result of direct numerical integration of the system (2.12), (2.13) with $\text{Pr} = 1$. Note that from the analysis $G'(0) = 0$ to the same order, a result which is also confirmed by direct numerical integration.

The local analysis given in this section is also applicable to the supercritical pitchfork and transcritical bifurcations at Ra, Ra_4, etc. providing the appropriate eigensolution is adopted. It can also be used to describe the solution in the vicinity of the subcritical pitchfork bifurcation at $\text{Ra}_{1,1}$ (and indeed at subsequent subcritical bifurcations); however, since the basic flow and eigensolution are only known by numerical integration, the appropriate integrals of this section must be determined numerically.

6. Conclusion

In this paper we have presented a body of results deduced from the sixth-order system of ordinary differential equations and from the associated temporal eigenvalue problem. We shall present results from the integration of the diffusion problem, as partially defined in (2.10) and (2.11), at a later stage.

Although the analytical and numerical methods involved are straightforward, the consequences of the results are considerable and varied. We are able to show analytically that the basic (stagnation) solution admits of bifurcations, of both pitchfork and transcritical types, and to infer the existence of both asymmetric and symmetric, but non-trivial, solutions. The existence of Hopf bifurcations and, as a result, of periodic solutions is inferred.

Although our results are theoretical, they do suggest consequences that experimenters (and, indeed, workers in the area of computational fluid dynamics on a finite x-interval) may find helpful when recording results. We are not aware of any results for the problem considered in this paper although in an experiment by Siegel and Norris [10] on the free convection between two heated vertical plates, asymmetric and unsteady flows were observed. However, no quantitative data were presented. There is, of course, no similarity solution possible for their problem and the full equations (see (2.1)–(2.3)) would have to be solved, a task requiring considerable computing power and time. This shows the benefit of a similarity solution like that considered here.

We remind the reader that our results are for two-dimensional configurations although clearly, in any attempt to verify certain of these predictions by experiment, the apparatus is of necessity three-dimensional – the length, L, of the channel in the Ox-direction and its width, $2H$, in the Oz-direction, are finite with possibly an open end at $x = L$ and walls at $z = \pm H$. In our analysis we have essentially assumed that h/L, h/H are sufficiently small that their effects on the solutions discussed above are negligible – at least in some restricted region of the channel. In our analysis we have exploited the Hiemenz similarity form to reduce the system of partial differential equations to a system of ordinary differential equations – a device that is useful but which loses some spatial structure. Further, the stability of the steady solutions has been examined within the confines of the Hiemenz form; such analysis does not preclude the existence of other instabilities, spatial or temporal.

There is one special case in which the effects of the bounding walls at $z = \pm H$ can be seen to have no effect on the known stable solution. If we arrange for these bounding walls to be

rigid and at the same temperature as the walls at $y = \pm h$, then for $-\infty < \mathrm{Ra} < \mathrm{Ra}_1$ the basic stagnation solution is still appropriate and, we can reasonably anticipate, stable. (The same result holds if the walls at $z = \pm H$ are insulating.)

However, in spite of these remarks, one should note that in a three-dimensional porous-channel investigation, Zaturska and Banks [11], it was found that the impermeable bounding (side) walls do affect the flow field at least in their vicinity.

Finally, we note that the configuration in which $x/L \ll 1$ but with the z-variation retained leads to a more complicated, but important, problem.

Appendix: $\mathrm{Pr} \neq 1$

The analysis presented in the body of the paper was based on the assumption of unit Prandtl number. The case for general values of Pr is not fundamentally different and we give some results here.

As already mentioned in §3, when $\mu = 1$ and $s = 0$ the eigenproblem (3.2) is independent of Pr. Consequently the values of Ra corresponding to zero eigenvalue (and trivial basic solution) will be the same as those of §3. We therefore deduce the important result that the values of Ra at which bifurcation points occur in the basic solution will be the same for all values of the Prandtl number.

We next consider the eigenvalues and eigenfunctions corresponding to asymmetric boundary conditions when $\mathrm{Ra} = 0$. The solution to the basic problem is then

$$F = F_0 = 0, \qquad G = G_0 = \tfrac{1}{2}(1 + \mu) - \tfrac{1}{2}(1 - \mu)y. \tag{A1}$$

The equation for the leading-order terms (θ_0, ϕ_0) when $\mathrm{Ra} = 0$ can therefore be written

$$\mathrm{Pr}^{-1}s\theta_0'' = \theta_0^{iv},$$

$$s\phi_0 + \tfrac{1}{2}\{(1 + \mu) - (1 - \mu)y\}\theta_0' + \tfrac{1}{2}(1 - \mu)\theta_0 = \phi_0'', \tag{A2}$$

with homogeneous boundary conditions on θ_0, θ_0' and ϕ_0 at $y = \pm 1$. We find, as in §3.2 when $\mathrm{Pr} = 1$, that there are three families of solutions: antisymmetric, symmetric and asymmetric modes. The first two families are as given in (3.13) and (3.14) while the asymmetric modes are given by

$$s_0 = -p^2 \,\mathrm{Pr}, \qquad \theta_0 = c(y \sin p - \sin py),$$

$$\phi_0 = c\{(1 + \mu)\phi_{01} + (1 - \mu)\phi_{02}\}, \tag{A3}$$

where $\tan p = p$, c is a normalising factor,

$$\phi_{01} = \tfrac{1}{2} \sec p\sqrt{\mathrm{Pr}} \{p^{-1}(1 - \mathrm{Pr})^{-1}(\cos py \cos p\sqrt{\mathrm{Pr}} - \cos p \cos p\sqrt{\mathrm{Pr}}y)$$

$$+ p^{-2} \mathrm{Pr}^{-1} \sin p(\cos p\sqrt{\mathrm{Pr}} - \cos p\sqrt{\mathrm{Pr}}y)\}$$

and

$$\phi_{02} = \{2p^2(\mathrm{Pr} - 1)\}^{-1}(py \cos py - \sin py)$$
$$+ \{p^2(\mathrm{Pr} - 1)^2 \sin p\sqrt{\mathrm{Pr}}\}^{-1}(\sin py \sin p\sqrt{\mathrm{Pr}} - \sin p \sin p\sqrt{\mathrm{Pr}}y).$$

We note, as in §3.2, that the antisymmetric and symmetric modes are independent of Pr and that the effect of Pr on the eigenvalue in the asymmetric modes is a multiplicative one. We also point out that if $\mathrm{Pr} \to 1$ in (A3) we recover (3.15), the analogous result when $\mathrm{Pr} = 1$.

It is of interest to note two limiting forms: for $0 < \mathrm{Pr} \ll 1$ we find that

$$\phi_{01} = \tfrac{1}{2}\{p^{-1}(\cos py - \cos p) + \tfrac{1}{2}(y^2 - 1) \sin p\},$$

(A4)

$$\phi_{02} = p^{-2}\{\tfrac{1}{2}(\sin py - py \cos py) + \sin py - y \sin p\},$$

while for $\mathrm{Pr} \gg 1$ we obtain the limiting behaviours

$$\phi_{01} \approx \frac{1}{2p\,\mathrm{Pr}}(\cos p - \cos py),$$

(A5)

$$\phi_{02} \approx \frac{1}{2p^2\,\mathrm{Pr}}(py \cos py - \sin py).$$

However, it will be seen that (A5) is not uniformly valid (e.g. the condition $\phi''(\pm 1) = 0$ is not satisfied by the limiting form for ϕ).

References

1. E.H.W. Schmidt, Heat transmission by natural convection at high centrifugal acceleration in water-cooled gas-turbine blades, Proc. General Discussion on Heat Transfer, Inst. M.E. and ASME, London, September 1951, pp. 361–363.
2. S.A.M. Said and R.J. Krane, An analytical and experimental investigation of natural convection heat transfer in vertical channels with a single obstruction, *Int. J. Heat Mass Transfer* 33 (1990) 1121–1134.
3. M.J. Lighthill, Theoretical considerations on free convection in tubes, *Quart. J. Mech. Appl. Math.* V1 (1953) 398–439.
4. S. Ostrach and P.R. Thornton, On the stagnation of natural-convection flows in closed-end tubes, *Trans. ASME* 80 (1958) 363–366.
5. M.B. Zaturska, P.G. Drazin and W.H.H. Banks, On the flow of a viscous fluid driven along a channel by suction at porous walls, *Fluid Dyn. Res.* 4 (1988) 151–178.
6. E.B.B. Watson, W.H.H. Banks, M.B. Zaturska and P.G. Drazin, On transition to chaos in two-dimensional channel flow symmetrically driven by accelerating walls, *J. Fluid Mech.* 212 (1990) 451–485.
7. M. Abramowitz and I.A. Stegun, *Handbook of Mathematical Functions*. National Bureau of Standards, Washington (1964).
8. J. Guckenheimer and P. Holmes, *Nonlinear Oscillations, Dynamical Systems, and Bifurcations of Vector Fields*. Springer-Verlag, New York (1986).
9. P. Watson, W.H.H. Banks, M.B. Zaturska and P.G. Drazin, Laminar channel flow driven by accelerating walls, *Eur. J. Appl. Math.* (in press).
10. R. Siegel and R.H. Norris, Tests of free convection in a partially enclosed space between two heated vertical plates, *Trans. ASME* 79 (1957) 663–673.
11. M.B. Zaturska and W.H.H. Banks, Suction-driven flow in a finite wedge, *Acta Mechanica* 86 (1991) 95–101.